Earthq Eng & Eng Vib (2009) 8: 459-467 **DOI**: 10.1007/s11803-009-9058-8

Engineering vibration monitoring by GPS: long duration records

F. Casciati† and C. Fuggini‡

Department of Structural Mechanics, University of Pavia, Italy

Abstract: Monitoring the performance of any structure requires real-time measurements of the change of position of critical points. Different techniques can be used for this purpose, each one offering advantages and disadvantages. The technique based on satellite positioning systems (GPS, GLONASS and the future GALILEO) seems to be very promising at least for long period structures. The GPS in particular provides sampling rates that are able to track dynamic displacements with high accuracy. Its service ability is independent of atmospheric conditions, temperature variations and visibility of the monitored object. This paper investigates the reliability and accuracy of the measurements of dual frequency GPS receivers. A linear electromagnetic motor moves an object along a given direction. The changes of position are compared with their estimates as recorded by a GPS receiver, whose antenna is located on the reference object. The comparison is based on sufficiently long records.

Keywords: infrastructure monitoring; global positioning system (GPS); delay; positioning errors; multi-path error; signal geometric dilution of precision; linear motor amplitudes; power spectral densities

1 Introduction

In civil infrastructure monitoring, the use of terrestrial positioning systems, such as laser displacement sensors, is incompatible with negative atmospheric conditions or large temperature variations.

The global navigation satellites systems (GNSS) have been proved to be useful for monitoring applications in structural engineering. The American Global Positioning System (GPS) is becoming an alternative to common accelerometers to measure the dynamic response of long-period structures (Celebi, 2000; Nickitopoulou *et al*., 2006; Kijewsji-Correa *et al*., 2006; Li *et al*., 2006; Psimoulis *et al*., 2008). The high-precision GPS technology has been used to monitor the wind-induced deformation of tall flexible buildings (Kijewsji-Correa and Kareem, 2003; Campbell *et al*., 2006; Seco *et al*., 2007; Hristopulos *et al*., 2007), to assess the vibrations of suspension and cable-stayed bridges (Xu *et al*., 2002; Lekidis *et al*., 2005), the displacements of high chimneys (Breuer *et al*., 2002) and large dams (Barnes and Cranenbroeck, 2006; Cazzaniga and Pinto, 2006). Many applications were developed by installing GPS receivers at key locations of the structure to capture their static and dynamic displacements in real-time and in all weather conditions (Tamura *et al*., 2002). In other cases, the GPS was incorporated in the monitoring of a major suspension bridge (Wong, 2004), or of tall structures (Psimoulis and Stiros, 2008).

The GPS guarantees its operability in all weather conditions and offers continuous long term acquisitions.

A real-time structural health monitoring system requires the absolute displacements of critical points to be collected. The relative displacements are then the key to assess drift and stress conditions in a structure. The GPS provides absolute displacements directly, without single or double integrations, as velocimeters and accelerometers require, thus removing all the problems related to the integration process (i.e., selection of filters, baseline correction, constants of integration, etc.).

In this study, the accuracy of GPS measurements is assessed by testing a GPS system made by a fixed reference receiver and a rover. The latest one moves along rails driven by a linear motor. The aim is to simulate harmonic displacements with the rover GPS receiver moving in the horizontal plane. By comparing the recorded coordinates of the receiver with the known parameters of the motor movements, the accuracy of the entire acquisition system can be verified.

2 Governing relationships

GPS positions are calculated using the concept of triangulation. The known position of overhead satellites allows the position of a GPS receiver/antenna pair on the Earth (Fig. 1) to be determined. Each satellite continuously transmits the current time kept by its atomic clock, as well as its current position x^j, y^j, z^j along its orbital path. The distance r_i^j of the jth satellite to the

Correspondence to: Fabio Casciati, Department of Structural Mechanics, Via Ferrata 1, 27100, Pavia, Italy
Tel: +39 0382 995465
E-mail: fabio@dipmec.unipv.it
†Professor; ‡PhD Student

Supported by: A Grant from the University of Pavia (FAR 2009)
Received April 7, 2009; **Accepted** June 15, 2009

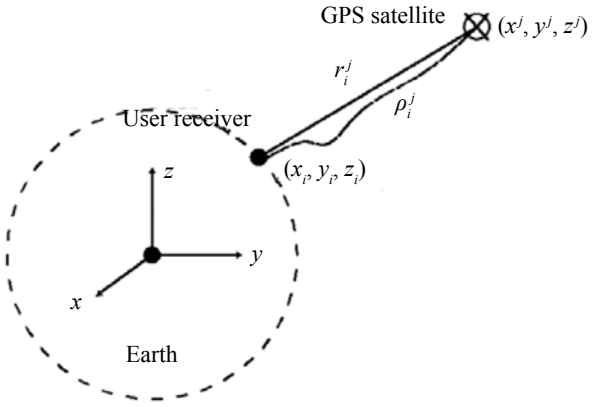

Fig. 1 Satellite – receiver distance

unknown position of the receiver on the Earth, x_i, y_i, z_i is computed by measuring the propagation time (Δt_i^j) required to move from the satellite to the user receiver antenna.

The coordinates x_i, y_i, z_i, of a static or moving receiver can be obtained in a static mode (a GPS antenna is fixed in a certain position and receives the information sent by a number of tracked satellites) or in a differential kinematic mode. In the latter case, the signal recorded by a moving receiver (rover) is corrected, in real-time or in post-processing, by a stationary receiver (reference) fixed in a nearby position.

In an ideal case, the true (i.e., geometric) satellite-to-receiver distance can be computed by multiplying the propagation time Δt_i^j by the speed of the light (c = 290,000 km/s). The distance r_i^j for any j (j = 1,2,... $N_{\text{satellites}}$) can be written as:

$$r_i^j = c\Delta t_i^j = c\left(T_i - T^j\right) = \sqrt{\left(x^j - x_i\right)^2 + \left(y^j - y_i\right)^2 + \left(z^j - z_i\right)^2} \tag{1}$$

where T_i represents the time at which the signal reaches the receiver, and T^j is the time at which the signal leaves the receiver. However, the satellite and receiver clocks are not perfectly synchronized. Thus, the satellite-to-receiver distance can be computed by introducing the distance $\bar{r}_i^j$ which is the sum of two terms: (i) the geometric range and (ii) an offset due to the difference between the reference time and the receiver clock:

$$\bar{r}_i^j = r_i^j + c\delta t_i^j \tag{2}$$

where δt_i^j represents the offset of the receiver clock. The satellite-to-receiver measurements are also corrupted by independent errors such as uncorrected satellite ephemeris and multipath. These errors are regarded as satellite signal delays to be added in Eq. (2) as:

$$\rho_i^j = \bar{r}_i^j + \varepsilon_i^j = r_i^j + c\delta t_i^j + \varepsilon_i^j = r_i^j + c\left(\delta t_i^j + \delta t_{\text{D}}\right) = r_i^j + c\left(\delta t_i^j + \delta t_{\text{atm}} + \delta t_{\text{m}} + \delta t_{\text{r}}\right) \tag{3}$$

Equation (3) represents a fictitiously increasing distance that is usually referred to as "pseudo-range satellite-receiver". Furthermore, in Eq. (3) δt_{D} is the signal delay producing a total time offset, resulting from the following effects: δt_{atm} which represents the delays due to atmosphere (i.e., ionospheric effects and tropospheric delay); δt_{m} multipath offset, δt_{r} receiver noises and hardware offset.

To make the terms in Eq. (3) explicit, the different sources of positioning errors, which are expressed as a signal delay, must be separated.

Equation (3) can be solved for the unknown terms by employing either (i) closed form solutions, (ii) iterative techniques based on linearization, or (iii) Kalman filtering. The linearization technique is adopted by the software.

The atmospheric effects, summarized in δt_{atm}, can be computed by separating its two components: the ionospheric delay and the tropospheric delay. Since the ionospheric delay is frequency dependent, it can be removed by exploiting dual-frequency (L_1 and L_2, which are the two carrier frequencies that transmit the GPS signal) GPS receivers. Note that the atmospheric error is strictly related to the adopted baseline (distance reference-rover): when the two antennas are close (say some meters) to each other, the ionospheric delay is the same for the reference and the rover, and hence the the error can be neglected. The tropospheric delay is not, on the contrary, frequency dependent and can be only reduced by considering a computational model such as the Hopfield scheme (Hopfield, 1969).

The multi-path error (which is difficult to remove within urban zones) is the result of a signal arriving at the receiver with a slight delay δt_{m} because it was reflected off by objects; that is, obstructing the line-of-sight from the satellite to the receiver.

Due to the δt_{D} errors producing a signal delay, the position (x_i, y_i, z_i) of a receiver can be computed by detecting at least four of the satellites available in the sky.

To summarize, the positions of the GPS antennas have to be chosen to satisfy the following requirements: (i) the antennas must have a clear view of the sky above to track the orbiting satellites, and (ii) the reference and the rover should be in close proximity to minimize baseline errors.

In addition, the quality of the GPS position estimates depends on the number and geometric distribution of available satellites.

Equation (3) contains an error term (ε_i^j) to which one associates a deterministic feature to the extent that it is expressed as a fictitious extra-time-delay, i.e., a single value for a given receiver.

It should be time dependent during a single day, since the satellites are not geo-stationary. This suggests that the estimate should be regarded as extracted by a population with mean and standard deviation; their values can be obtained from a record of one or more days.

However, the repetition day after day is affected by uncertainties and this further aspect is known in the

literature (Leick 1995) as "signal geometric dilution of precision" (GDOP), which is mainly due to a deviation from the idealized geometric distribution of satellites.

The GDOP is modelled as a geometric factor that describes the effect of the actual geometric satellite distribution on the accuracy of the position solution. From an analytical point of view, GDOP represents the amplification of the standard deviation of the measurement errors.

In others words, the standard deviation (σ) of the "pseudo-range" (ρ_i^j) is affected by a factor, f_{GDOP}, that allows the corrected standard deviation of the "pseudo-range" $\overline{\sigma}\left(\rho_i^j\right)$ to be obtained as a function of the geometric satellite configuration, as shown in Eq. (4):

$$\overline{\sigma}\left(\rho_i^j\right) = \sigma\left(\rho_i^j\right) \cdot f_{\mathrm{GDOP}} \tag{4}$$

GDOP is inherent in the satellite technology and can be removed only by adding further satellites.

3 Experimental mock-up

The system architecture is made up of an outdoor part, the antennas (6.2 cm height, 17.0 cm of diameter, 0.4 kg weight) and an indoor part, the receivers and a computer running two Leica software products.

The devices which were installed are (Leica, 2005):

- a dual frequency high precision Leica GMX902 GPS receiver, working as a reference, with a maximum sampling rate of 20 Hz;
- a dual frequency high precision Leica GMX902 GPS receiver, working as a rover, with a maximum sampling rate of 20 Hz;
- two dual frequency Leica AX1202 antennas, recording signal with a sampling rate up to 20 Hz.

The GPS signals are recorded by the Leica GPS Spider software that furnishes information on the configuration of the satellites and allows data corrections for real-time positioning. The recorded displacement signals are then analyzed using a system identification toolbox (Matlab, 2004).

The two GPS antennas were anchored on a stiff concrete surface in an open field location and in a position that is guaranteed to track a minimum of six satellites during the day.

Two scenarios were conceived. First, the two antennas were placed on a concrete block at a height of around 3 m near an industrial steel building in Pavia (Casciati *et al.*, 2008). In a second experimental campaign, the antennas were located on the roof of the same industrial building at the height of about 11 m and at a distance of 13 m.

The first case, with the GPS antennas placed at a height of 3 m next to the steel building, was used to calibrate the resolution of the GPS system in acquiring known and fixed longitudinal displacements. Many tests were conducted and the results showed an interesting and promising agreement with the imposed displacements. The idea was to install the moved antenna on a Linmot linear motor (Fig. 2). The linear motor moves, following assigned displacement time histories of different amplitudes and periods, through a software program. The antenna fixed on the moving part of the motor is forced to move to a known position, along the direction of the linear motor, working in the horizontal plane. The coordinates of the point where the antenna is fixed are recorded by the rover receiver. They can then be compared with the change of position imposed by the linear motor.

The main conclusion achieved by the first GPS network set-up is summarized as follows.

The tests carried out were influenced by the poor localization of the GPS antennas. In fact, the position near the steel building does not completely satisfy the requirement of a clear view of the sky above the antennas and this led to instantaneous loss of signal. Therefore, the achieved results were sometimes very good, sometimes not very good (in terms of precision), and other times no data were recorded at all when the building was obstructing its view.

This suggests that a different location of the sensors should be identified, that would be able to provide open sky conditions above the sensors and continuous reception of the satellite signal.

In the new arrangement, the antennas were placed on the roof of the industrial steel building in an open field environment, free from sources of multi-path errors and from buildings that may obstruct the view of the low elevation satellites (those that formed an angle with the horizon of around 15°–30°). The antennas were linked to their receivers by wire connections, with other wires connecting the receivers to a computer for acquisition of the GPS signals. Dual frequency L_1/L_2 GPS receivers were used to guarantee the maximum achievable accuracy. The rover and the reference receivers communicated each to the other to allow the

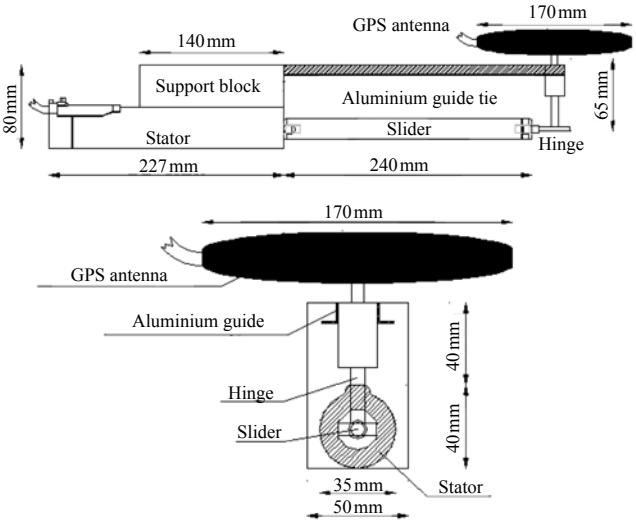

Fig. 2 Lateral (top) and frontal (bottom) view of the linear motor with the rover antenna

correction of position errors. For this purpose, the *GPS Differential Point Positioning (DGPS)* is used (Dana, 1997). The correct position of the reference is sent via a wire connection to acquisition software, that acquires the coordinates and information from the reference position in real-time, computes new coordinates and transmits the correction of the position to the rover. This positioning allows the rover errors of position to be removed and the correct position to be obtained within a resolution of sub-centimetres.

4 Experimental results

Two types of tests were carried out to collect all possible information needed to assess the achievable accuracy of the GPS units for long-term precise monitoring applications: static and dynamic.

Static tests were carried out to quantify the background noise in the GPS configuration, and to investigate the influence of GDOP on the recorded signal. The tests provide answers to two main questions: a) repeatability of long-period oscillations in both the longitudinal and transversal directions for two consecutive satellite configurations; and b) evaluation of the best resolution possible when adopting dual frequency GPS receivers.

Dynamic tests were designed to quantify the range of frequencies and amplitudes that can be successfully tracked by GPS sensors in civil engineering applications.

4.1 Static tests

Some preliminary static calibration tests were carried out to assess the performance and stability of the *DGPS* system when no motion was imposed on the movable antenna. This phase allows the background noise in the GPS configuration to be quantified and, within 48 hours of acquisition, the influence of the GDOP on the recorded signal can also be quantified. The experiments were conducted using two GPS antennas that stayed in a known position for about two consecutive days. The GPS sampling rate was chosen to be 10 Hz.

Since the full 24 h day registration is too long to be depicted, extracts of ten hours in the E-W direction, in the N-S direction and in the vertical direction are plotted in Fig. 3 over the two days.

The correlation between the values recorded at instants shifted of 24 h can be studied. For all three components, a strong correlation between the two days peaks is made evident.

Figure 4 shows the correlation between the two days in the East, North and vertical directions. In these tests, relative motions along the N axis are marked as ΔN, while those along the E axis as ΔE; those along the vertical axis are marked as ΔH.

Note that the East component is also reported as the longitudinal component in this paper, and the North component as the transversal one.

The three root means square (RMS) values corresponding to the East, North and vertical components of displacements, respectively, for the two days were also calculated. Table 1 summarizes these values, which can be considered as the radii of rms ellipses.

The simultaneous couple (ΔN, ΔE) are collected in the diagram on Fig. 5, where the ellipse with a radius of two root mean square (RMS) values is also drawn. It denotes a slightly lower level of accuracy in the North direction than along the East direction. For this reason, in the dynamic tests, the longitudinal component of the motion is directed along the East direction.

A power spectral analysis of the recorded time histories was also carried out to compare the frequency content over two consecutive days for the East, North and vertical components. In Fig. 6, the PSDs for the three directions are plotted. Note that for the three components and the two days, the PSD of the recorded displacements shows a nearly white noise spectrum.

The test is repeated by selecting the baseline along the North direction. The results are plotted in Fig. 7, which shows a slightly better resolution along the North direction than in Fig. 5.

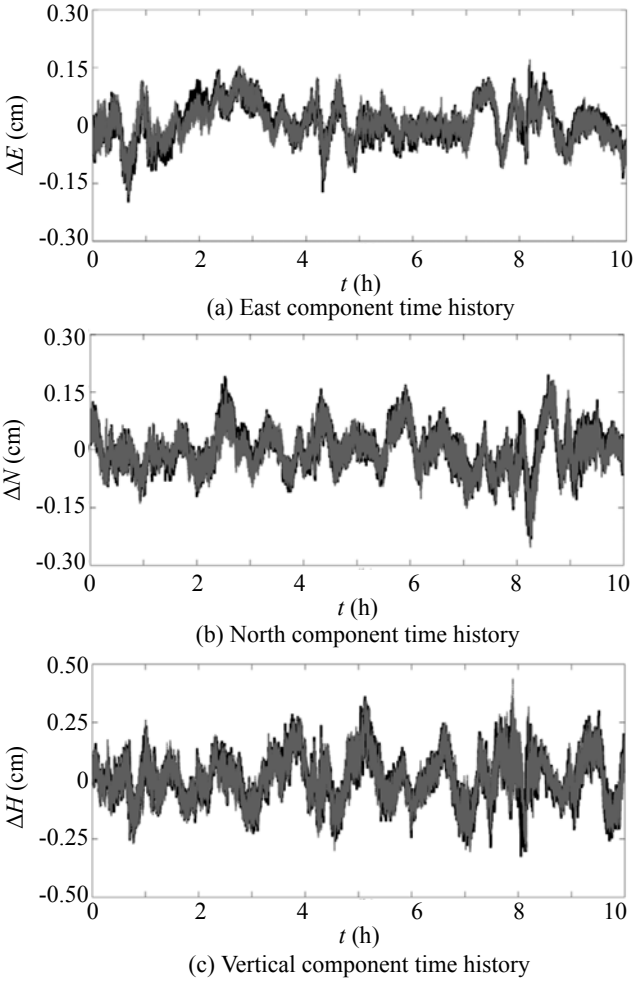

Fig. 3 Correlation between two consecutive days (day 1 in black and day 2 in grey)

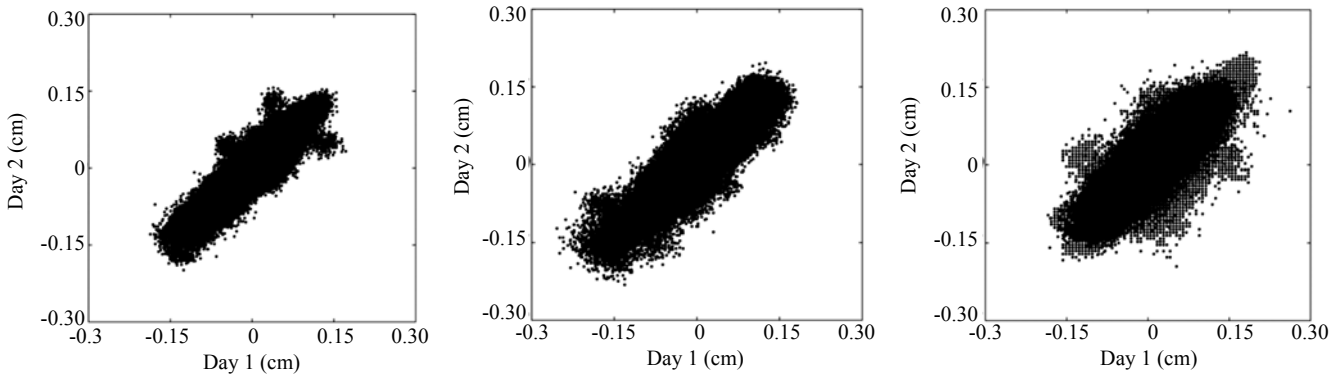

Fig. 4 Correlation between days: East component response (left); North component response (middle); Vertical component response (right)

Table 1 RMS values of the North, East and vertical components for two consecutive days

	Day 1 RMS	Day 2 RMS	Difference RMS
East	0.0465 cm	0.048 cm	4.2%
North	0.0494 cm	0.0506 cm	2.5%
Height	0.0927 cm	0.0935 cm	0.9%

4.2 Dynamic tests

Dynamic calibration tests were designed to quantify the range of frequencies and amplitudes that can be successfully tracked by dual frequency GPS receivers. The dynamic tests were carried out for different combinations of frequency and amplitude by imposing sinusoidal time histories on the linear motor. In particular, attention is focused on a frequency range of oscillations lower than 4 Hz, which is typical of the main modal frequencies of large engineering structures (i.e., high-rise buildings, suspension bridges, etc.). The recorded coordinates of the moving receiver are processed and then compared with the real values of the linear motor movement. The GPS raw data were recorded in real-time by the Leica GPS software and then processed into the Matlab environment.

The amplitudes of the oscillations imposed on the

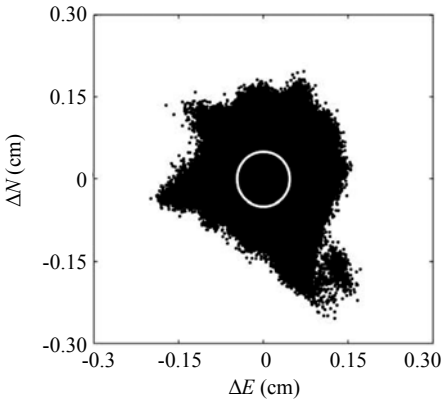

Fig. 5 Correlation between E-N components during two consecutive days with the calculated E-N RMS in white

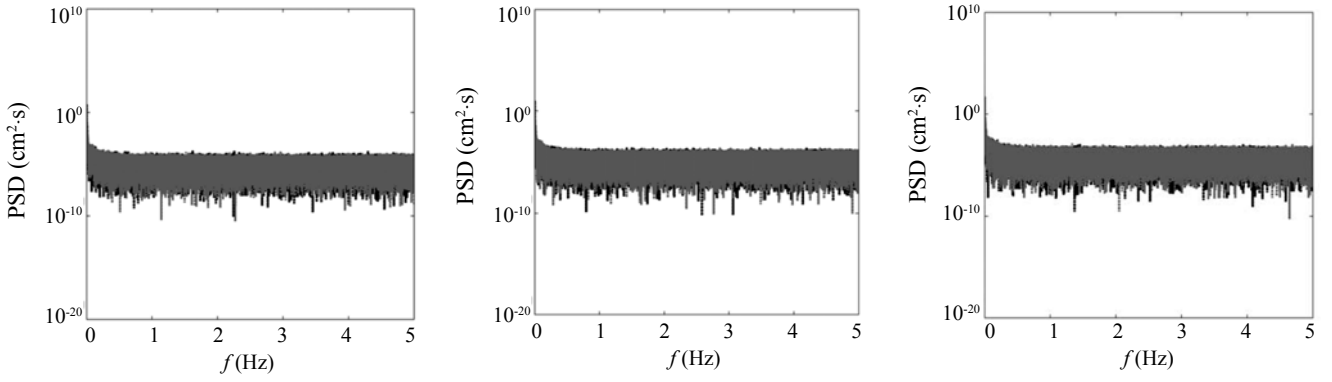

Fig. 6 Power spectral density function: East component (left), North component (middle); Vertical component (right)

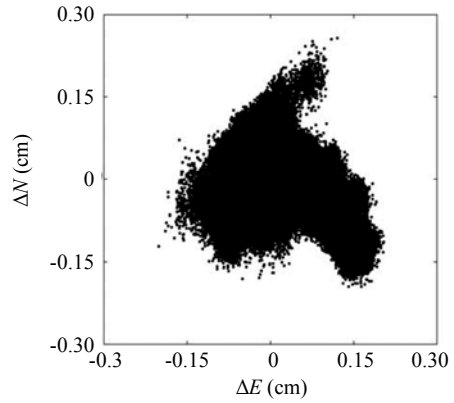

Fig. 7 Correlation between E-N components over two consecutive days

moving GPS antenna vary in a range from ±0.5 cm up to ±5 cm with frequencies of 0.1; 0.2; 0.5; 1; 2 Hz. The time history of any possible combination of these parameters has the duration of 300 s, assumed to be long enough to assess the stability of the measurements. Note that the data comparison was made with real linear motor longitudinal movements, as the actual imposed displacements are not always the same as those that are assigned.

Preliminary dynamic tests were carried out by imposing sudden variations of movement in amplitudes and frequencies to the linear motor. In these tests, the sampling rate was chosen to be 20 Hz.

In Figs. 8 and 9, two displacement time history records of uni-axial ΔL motion are plotted, showing the behavior of the rover GPS in response to these sudden variations in the linear motor displacements. In particular, in Fig. 8, both the frequency (with values of 0.2, 0.5 and 1 Hz) and the amplitude (from 1 to 12.5 cm) were varied, while in Fig. 9 only the amplitude was changed in a range from 1 to 10 cm, maintaining a fixed frequency of 0.5 Hz. The two power spectral density diagrams are plotted at the bottom of Figs. 8 and 9. In Fig. 8, the frequencies of 0.2, 0.5 and 1 Hz are clearly detected, while in Fig. 9, the PSD only shows the frequency of 0.5 Hz.

Two main considerations were seen in the plotted diagram: (i) the GPS was able to follow sudden changes in the displacement amplitudes; and (ii) the GPS was able to detect the change in frequencies that occurred in a short time period.

The dynamic tests were carried out by varying the amplitudes and the frequencies of the motion. The sampling rate was chosen to be 10 Hz.

As the entire tests were too long to be reported, a synthesis is presented in terms of (i) displacement time series; (ii) root mean square variations with time; and (iii) power spectra density changes with time.

The three plots in each subplot of Fig. 10 show

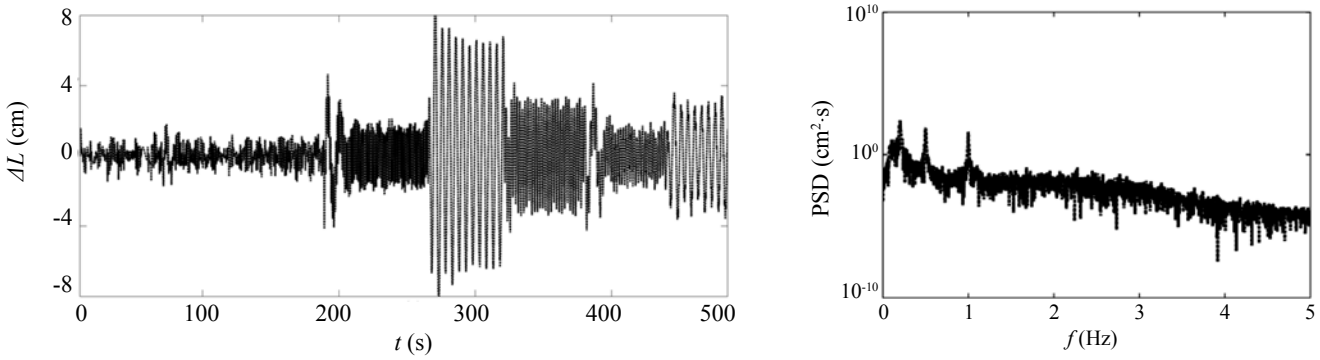

Fig. 8 GPS longitudinal displacement time history with frequencies 0.2, 0.5 and1 Hz and amplitudes 1–12.5 cm (left); corresponding PSD (right)

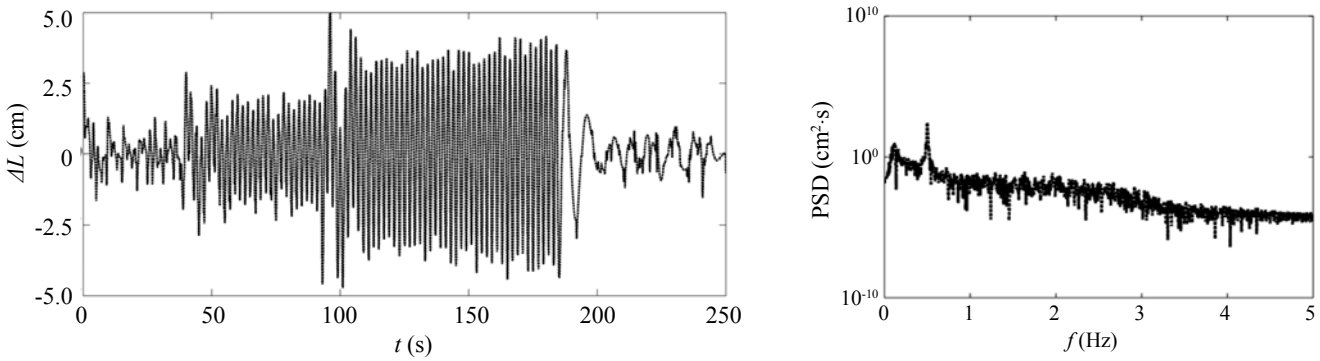

Fig. 9 GPS longitudinal displacement time history with frequency 0.5 Hz and amplitudes 1–10 cm (left); corresponding PSD (right)

the time history and the variation in time of an rms measurement and the associated power spectral density (PSD) function, respectively.

The comparison between the displacement estimates recorded by the GPS moving receiver and the displacements recorded by the linear motor is shown in the first graph. The rms values of the second plot are calculated as the rms of the ratio between the GPS estimate and the motor displacement at each instant, for each 60 s segment of the recorded time history. The PSD calculated in the third plot is computed for each separate 60 s segment of the recorded GPS and linear motor movements.

Figure 10 shows results from four tests with different

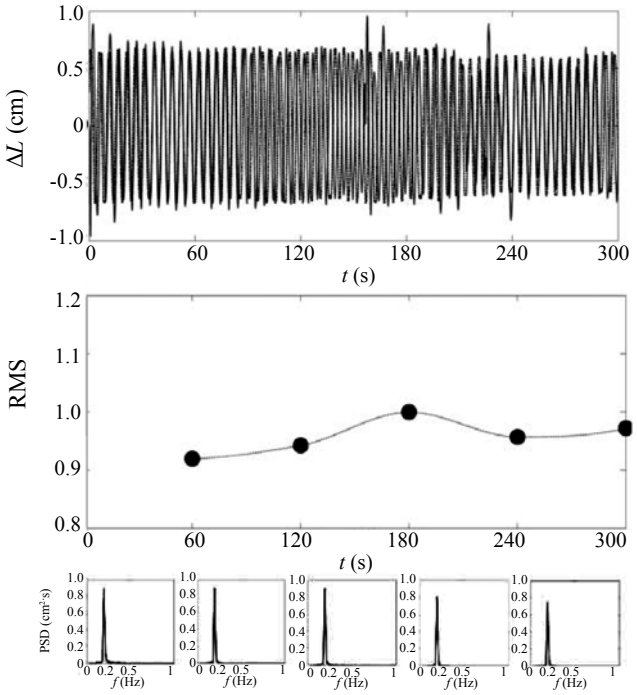

(a) Test with displacement amplitudes of ±0.75 cm and frequency of 0.2 Hz

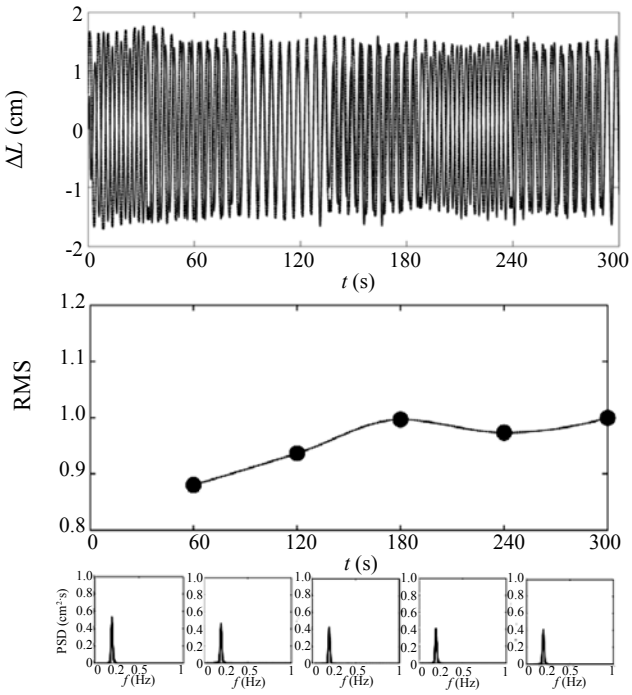

(b) Test with displacement amplitudes of ±1.75 cm and frequency of 0.2 Hz

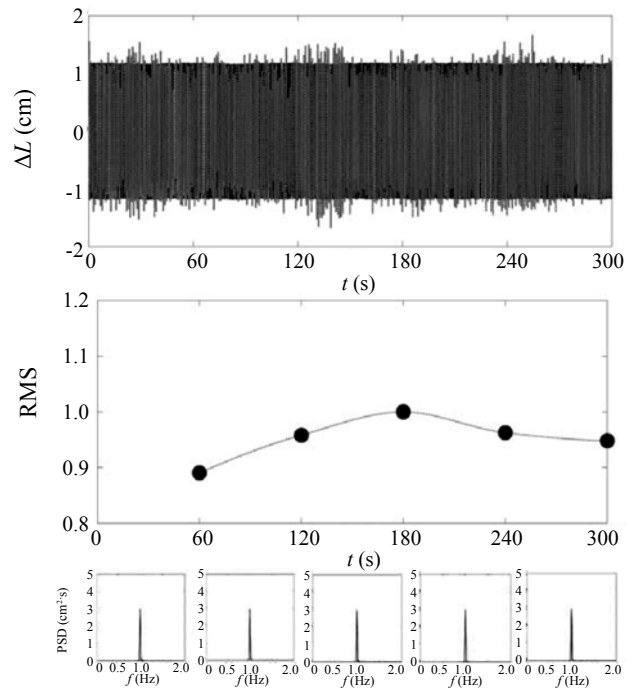

(c) Test with displacement amplitudes of ±1.25 cm and frequency of 1.0 Hz

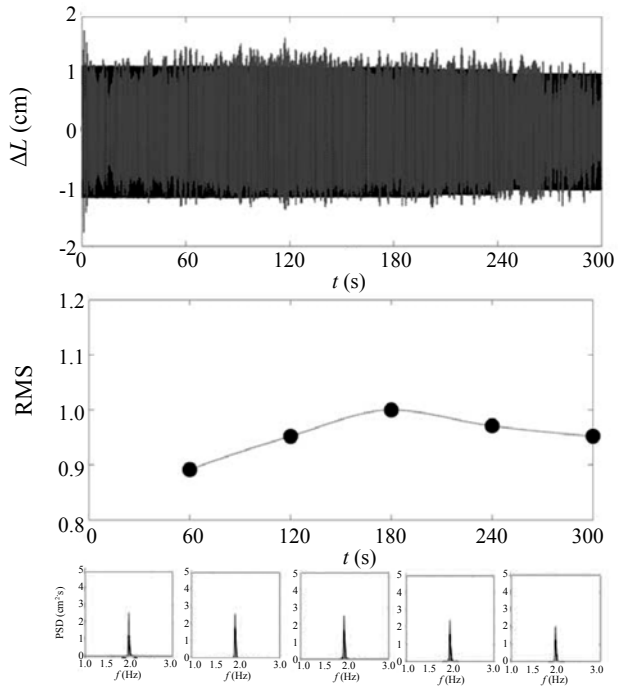

(d) Test with displacement amplitudes of ±1.25 cm and frequency of 2.0 Hz

Fig. 10 Results from dynamic tests: GPS (grey) and linear motor (black) displacements time history (top); variation in time of the rms of the ratio between GPS estimate and linear motor amplitudes (middle); corresponding GPS (grey) and linear motor (black) power spectral densities (PSD) (bottom)

displacement amplitude and frequency combinations. In all these figures, the middle plot, which reports the variation in the time of the rms of the ratio between the estimate and the motor displacement, shows an interesting trend of convergence in time. The trend is confirmed by similar plots for tests with different amplitudes and frequencies, but not illustrated here. Nevertheless, to formulate a conclusion based on these results requires further validation. The bottom plots show perfect agreement in the frequency domain.

A synthesis of the results is achieved with the plots in Fig. 11, where the ratio of the rms values is plotted versus the frequency and the amplitude.

The results plotted in Fig. 11 may appear as a negative feature for the GPS acquisition system.

Indeed, the equivalent plots for measurements collected with a non-contact laser sensor of good precision are collected in Fig. 12. The comparison confirms the better quality of the GPS measurements.

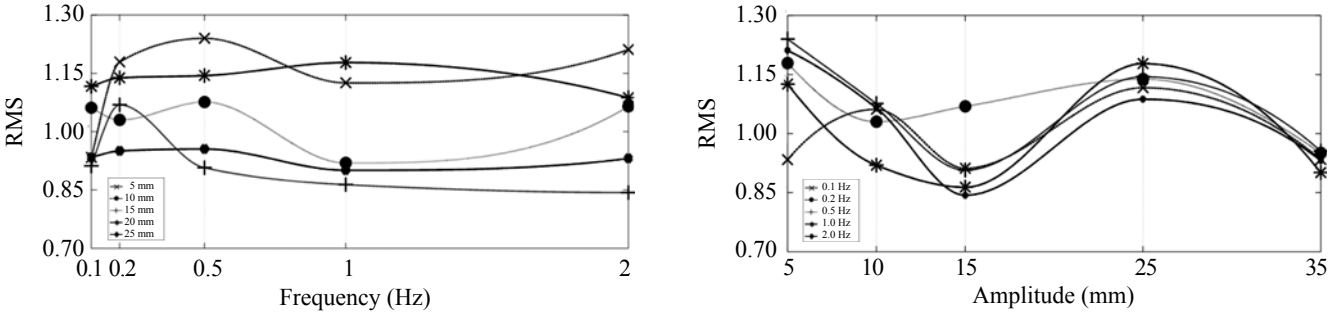

Fig. 11 Ratio between the RMS values computed along the entire record for the GPS estimate and the motor movements versus frequency (left) and amplitude (right) of oscillations

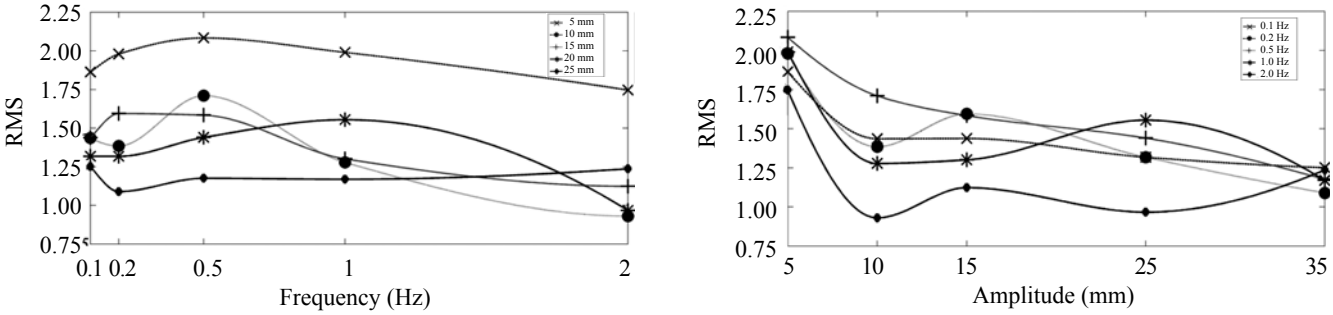

Fig. 12 Plots equivalent to Fig. 11 but achieved by measuring the displacement with a non-contact laser sensor

5 Conclusions

This paper discusses the level of accuracy that can be achieved by dual frequency GPS receivers to detect static and dynamic movements.

First, static tests were performed to quantify the geometric dilution of precision (GDOP) of the GPS measurements over two consecutive days (i.e., for two consecutive satellite configurations) and to assess the resolution that can be achieved. The static tests were conducted in an ideal environment, free from any external source of errors. The results show the accuracy of the GPS along the East, North and vertical directions. In particular, it is shown that the GPS measurements are more accurate for horizontal displacements than for vertical ones.

Dynamic tests were then performed to assess the precision of GPS measurements to detect and identify dynamic movements of different amplitudes and rates. Fixed longitudinal oscillations were imposed by a linear motor to a moving GPS receiver.

The major outcome of the study shows that the GPS allows displacements on the order of sub-centimeters to be monitored with frequencies of motion up to 2 Hz. Furthermore, the precision of the GPS depends on the combination of amplitude and rate of the imposed movements.

In conclusion, the test program confirms that the GPS is a promising tool in the field of civil engineering, and its accuracy is consistent with the monitoring requirements for flexible structures.

Acknowledgement

The authors acknowledge the GPS installation and

the technical support as provided by Leica Geosystems. The research was supported by a grant from the University of Pavia (FAR 2009).

References

Barnes J and Cranenbroeck J Van (2006), "The Potential of a Ground Based Transceivers Network for Water Dam Deformation Monitoring," *International Conference Hydropower*, Kunming, 23–25 October 2006, pp.765–795.

Breuer P, Chmielewski T, Gorski P and Konopka E (2002), "Application of GPS Technology to Measurements of Displacements of High-rise Structures Due to Weak Winds," *Journal of Wind Engineering and Industrial Aerodynamics,* **90**: 223–230.

Campbell S, Kwok KCS, Keung YL and Hitchcock PA (2006), "Full-scale Monitoring of a High-residential Building Using GPS Under Typhoon Conditions," *4th World Conference on Structural Control and Monitoring*, San Diego, 11–13 July 2006.

Casciati F, Fuggini C and Bonanno C (2008), "Dual Frequency GPS Receivers: Reliability of Precision of the Measures," *Proceedings 4ème Colloque en Interdisciplinaire en Instrumentation C2I*, 604–612, Hermes Science, Paris, France.

Cazzaniga NE and Pinto L (2006), "Structural Monitoring with GPS and Accelerometers: the Chimney of the Power Plant in Piacenza," *3rd IAG Symposium on Geodesy for Geotechnical and Structural Engineering and 12th FIG Symposium on Deformation Measurements*, Baden, 22–24 May 2006.

Celebi M (2000), "GPS in Dynamic Monitoring of Long-period Structures," *Soil Dynamics and Earthquake Engineering*, **20**: 477–483.

Dana PH (1997), "Global Positioning System (GPS) Time Dissemination for Real-time Applications, Real-time Systems," *The International Journal of Time Critical Computing Systems*, **12**: 9–40.

Hopfield HS (1969), "Two–quadratic Tropospheric Refractivity Profile for Correction Satellite Data," *Journal of Geophysical Research*, **7**(18): 4487–4499.

Hristopulos DT, Mertikas SP, Arhontakis I and Brownjohn JMW (2007), "Using GPS for Monitoring Tall-building Response to Wind Loading: Filtering of Abrupt Changes and Low-frequency Noise, Variography and Spectral Analysis of Displacements," *GPS Solutions*, **11**: 85–95.

Kijewsji-Correa TL and Kareem A (2003), "The Chicago Monitoring Project: a Fusion of Information Technologies and Advanced Sensing for Civil Infrastructures," *Proceedings of 1thInternational Conference on Structural Health Monitoring and Intelligent Infrastructure*, Tokyo, 13–15 November 2003, pp.1003–1010.

Kijewsji-Correa T, Kareem A and Kochly M (2006), "Experimental Verification and Full-scale Deployment of Global Positioning Systems to Monitor the Dynamic Response of Tall Buildings," *Journal of Structural Engineering*, **132(**8): 1242–1253.

Leica (2005), "GMX 902 User Manual", *Leica Geosystems AG*, 1–32.

Leick A (1995), *GPS Satellite Surveying*, New York: John Wiley & Sons, Inc .

Lekidis V, Tsakiria M, Makrab K, Karakostasb C, Klimisb N and Sous I (2005), "Evaluation of Dynamic Response and Local Soil Effects of the Evripos Cable-stayed Bridge Using Multi-sensor Monitoring Systems," *Engineering Geology*, **79**: 43–59.

Li X, Ge L, Ambikairajah E, Rizos C, Tamura Y and Yoshida A (2006), "Full-scale Structural Monitoring Using an Integrated GPS and Accelerometer System," *GPS Solutions*, **10**: 233–247.

Matlab (2004), The MathWork Inc., Version 7 (R14), 2004.

Meng X, Dodson AH and Roberts GW (2007), "Detecting Bridge Dynamics with GPS and Triaxial Accelerometers," *Engineering Structures*, **29**: 3178–3184.

Nickitopoulou A, Protopsalti K and Stiros S (2006), "Monitoring Dynamic and Quasi-static Deformations of Large Flexible Engineering Structures with GPS: Accuracy, Limitations and Promises," *Engineering Structures*, **28**: 1471-1482.

Psimoulis P, Pytharouli S, Karambalis D and Stiros S (2008), "Potential of Global Positioning System (GPS) to Measure the Frequencies of Oscillations of Engineering Structures," *Journal of Sound and Vibration*, **318**: 606–623.

Psimoulis P and Stiros S (2008), "Experimental Assessment of the Accuracy of GPS and RTS for the Determination of the Parameters of Oscillation of Major Structures," *Computer-Aided Civil and Infrastructure Engineering*, **23**: 389–403.

Seco A Tirapu F, Ramirez F, Garcia B and Cabrejas J (2007), "Assessing Building Displacement with GPS," *Building and Environment*, **42**: 393–399.

Tamura Y, Matsui M, Pagnini LC, Ishibashi R and Yoshida A (2002), "Measurement of Wind Induced Response of Building Using RTK-GPS," *Journal of Wind Engineering and Industrial Aerodynamics*, **90**: 1783–1793.

Wong KY (2004), "Instrumentation and Health Monitoring of Cable-supported Bridges," *Structural Control and Health Monitoring*, **11**: 91–124.

Xu L, Guo JJ and Jiang JJ (2002), "Time-frequency Analysis of a Suspension Bridge Based on GPS," *Journal of Sound and Vibration*, **254**(1): 105–116.